Nonlinear Controller for Stand-alone PV System

* Hassan Abouobaida
Department of Electrical Engineering,
Ecole Mohamadia d'ingénieur,
Mohamed V University,
Rabat, Morocco
Email: Hassan_abouobaida@yahoo.fr

Mohamed Cherkaoui
Department of Electrical Engineering,
Ecole Mohamadia d'ingénieur,
Mohamed V University,
Rabat, Morocco
Email: Cherkaoui@emi.ac.ma

Abd Elmonim El magri
Department of Electrical Engineering,
Ecole Mohamadia d'ingénieur,
Mohamed V University,
Rabat, Morocco
Email: el_maguiri@yahoo.fr

***Abstract*- The present work describes the analysis, modeling and control of a Boost-Buck power inverter used as a DC-DC and DC-AC power conditioning stage for autonomous photovoltaic (PV) systems.**

To maximize the steady-state input-output energy transfer ratio a backstepping controller is designed to produce balanced three phase voltage, extract and transfer a maximum Power extracted from photovoltaic generator. The achievement of the DC-AC conversion and the efficient PV's energy extraction are validated with simulation results.

Keywords: *MPPT, unity power factor, backstepping controller.*

I. Introduction

Many renewable energy technologies today are well developed, reliable, and cost competitive with the conventional fuel generators. The cost of renewable energy technologies is on a falling trend as demand and production increases. There are many renewable energy sources such as solar, biomass, wind, and tidal power. The solar energy has several advantages for instance clean, unlimited, and its potential to provide sustainable electricity in area not served by the conventional power grid.

However, the solar energy produces the dc power, and hence power electronics and control equipment are required to convert dc to ac power. There are two types of the solar energy system; stand-alone power system and grid-connected power system. Both systems have several similarities, but are different in terms of control functions. The stand-alone system is used in off-grid application with battery storage. Its control algorithm must have an ability of bidirectional operation, which is battery charging and inverting. The grid-connected system, on the other hand, inverts dc to ac and transfers electrical energy directly to power grid. Its control function must follow the voltage and frequency of the utility-generated power presented on the distribution line. With a GCI (grid connected inverter) excess power is bought and credited by the utility, and grid power is available at times when the local demand exceeds the PV system output [1].

In stand-alone system, a power conditioning system linking the solar array and the load is needed to facilitate an efficient energy transfer between them, this implies that the power stage has to be able to extract the maximum amount of energy from the PV and produce balanced three phase voltage with low harmonic distortion and robustness in front of system's perturbations.

In order to extract the maximum amount of energy the PV system must be capable of tracking the solar array's maximum power point (MPP) that varies with the solar radiation value and temperature. Several MPPT algorithms have been proposed, namely, Perturb and Observe (P&O) [2], incremental conductance [3], fuzzy based algorithms, etc. They differ from its complexity and tracking accuracy but they all required sensing the PV current and/or the PV voltage [4].

In this paper, a backstepping control strategy is developed to extract and transfer maximum power of a solar generating system and to produce balanced three phase voltage to supply the load [5]. The desired array voltage is designed online using a P&O (Perturb and Observe) MPP tracking algorithm. The proposed strategy ensures that the MPP is determined and the system errors are globally asymptotically stable. The stability of the control algorithm is verified by Lyapunov analysis.

The rest of the paper is organized as follows. The dynamic model of the global system (GPV, boost converter and buck inverter) are described in Section II. A backstepping controller is designed along with the corresponding closed-loop error system and the stability analysis is discussed in Section III. In Section IV, a simulation results proves the robustness of the controller with respect solar radiation and temperature change.

II. MPPT System Modeling

The solar generation model consists of a PV array module, dc-to-dc boost converter and a dc-to-ac inverter as shown in Figure 1.

A. PV model

PV array is a p-n junction semiconductor, which converts light into electricity. When the incoming solar energy exceeds the band-gap energy of the module, photons are absorbed by materials to generate electricity. The equivalent-circuit model of PV is shown in Figure 2. It consists of a light-generated source, diode, series and parallel resistances [6]-[7].

B. BOOST model

The dynamic model of the PV generator and the boost converter illustrated in figure 3 can be expressed by an instantaneous switched model as follows [5]:

$$c_1.\dot{u}_{pv} = i_{pv} - i_{L1} \tag{1}$$

$$L_1.\dot{i}_{L1} = u_{pv} - (1 - u_0).v_b \tag{2}$$

Where L_1 and i_{L1} represents the dc-to-dc converter storage inductance and the current across it, v_b is the battery voltage and u_0 is the switched control signal that can only take the discrete values 0 (switch open) and 1 (switch closed).

Using the state averaging method, the switched model can be redefined by the average PWM model as follows:

$$c_1.\dot{\bar{u}}_{pv} = \bar{i}_{pv} - \bar{i}_{L1} \tag{3}$$

$$L.\dot{\bar{i}}_{L1} = \bar{u}_{pv} - \alpha_0.\bar{v}_b \tag{4}$$

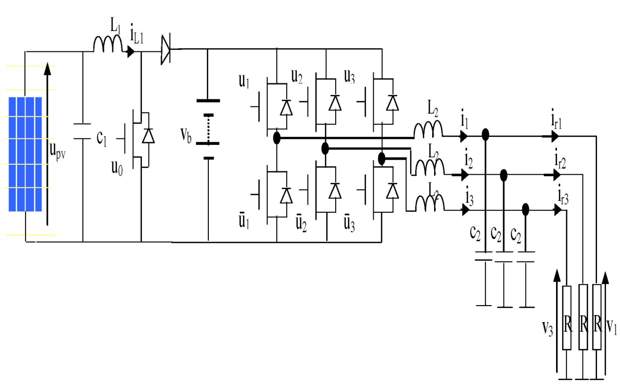

Fig. 1. Cascade connection of a boost converter with a full-bridge inverter

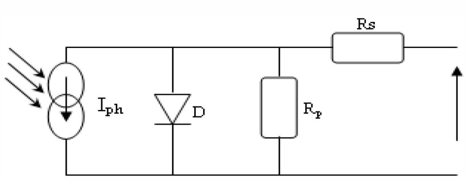

Fig.2 Equivalent model of PV Generator

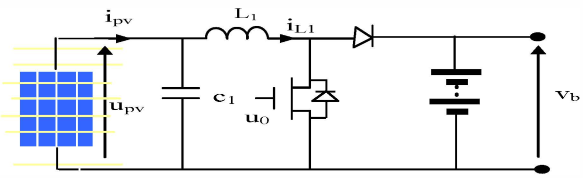

Fig 3. PV array connected to boost converter

Where α_0 is averaging value of u_0 -1, $\bar{u}_{pv}$ and $\bar{i}_{pv}$ are the average states of the output voltage and current of the PV generator, $\bar{i}_{L1}$ is the average state of the inductor current.

C. Inverter model

The active power transfer from the PV panels is accomplished by regulating the voltage that supply the load. The inverter operates as a voltage-control inverter (VCI). Noticing that u_k stand for the control signal of the inverter, the system can be represented by differential equations:

$$c_2.\dot{v}_k = i_k - i_{rk} \tag{5}$$

$$L_2.\dot{i}_k = v_{sk} - v_k - v_{nm} \tag{6}$$

$$v_{sk} = u_k.\mathrm{v}_b \tag{7}$$

Where v_b, v_{sk}, v_k designs a battery voltage, output inverter voltage and load voltage respectively. And i_k, i_{rk} are inverter output current and load current respectively.

Using the state averaging method (on cutting period), the switched model can be redefined by the average PWM model as follows:

$$c_2.\dot{\bar{v}}_k = \bar{i}_k - \bar{i}_{rk} \tag{8}$$

$$L_2.\dot{\bar{i}}_k = \bar{v}_{sk} - \bar{v}_k - \bar{v}_{nm} \quad \text{(k=1, 2, 3)} \tag{9}$$

$$\bar{v}_{sk} = \alpha_k.\bar{v}_b \tag{10}$$

Where α_k is averaging value of u_k

III. Design of non-linear controller

The backstepping approach is a recursive design methodology. It involves a systematic construction of both feedback control laws and associated Lyapunov functions. The controller design is completed in a number of steps, which is never higher than the system order.

Two main objectives have to be fulfilled in order to transfer efficiently the photovoltaic generated energy into the resistive load are tracking the P's maximum power point (MPP) and regulate the output voltage. Figure 4 shows the control scheme used to accomplish the previous objectives [8].

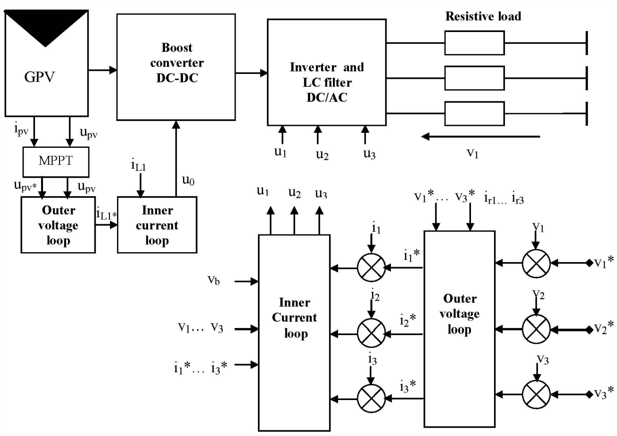

Fig. 4 Control scheme

A. *Control of Boost converter*

The boost converter is governed by control signal u_0 generated by a backstepping controller that allow to extract maximum of photovoltaic generator control by regulating the voltage of the photovoltaic generator to its reference provided by conventional P&O MPPT algorithm.

Step 1. Let us introduce the input error:

$$e_1 = u_{pv} - u_{pv}^* \tag{11}$$

Deriving e_1 with respect to time and accounting for (3), implies:

$$\dot{e}_1 = \dot{u}_{pv} - \dot{u}_{pv}^* = \dot{u}_{pv} - \left(\frac{i_{pv}}{c_1} - \frac{i_{L_1}}{c_1}\right) \tag{12}$$

In equation (12), i_{L1} behaves as a virtual control input. Such an equation shows that one gets $\dot{e}_1 = -k_1.e_1$ ($k_1 > 0$ being a design parameter) provided that:

$$i_{L_1} = -k_1.c_1.e_1 + i_{pv} - c_1.\dot{u}_{pv}^* \tag{13}$$

As i_{L1} is just a variable and not (an effective) control input, (12) cannot be enforced for all $t \geq 0$. Nevertheless, equation (12) shows that the desired value for the variable i_{L1} is:

$$\beta_1 = i_{L_1}^* = -k_1.c_1.e_1 + \bar{i}_{pv} - c_1.\dot{u}_{pv}^* \qquad 4)$$

Indeed, if the error:

$$e_2 = i_{L_1} - i_{L_1}^* \tag{15}$$

vanishes (asymptotically) then control objective is achieved i.e. $e_1 = u_{pv} - u_{pv}^*$ vanishes in turn. The desired value β_1 is called a stabilization function.

Now, replacing i_{L1} by $(e_2 + i_{L1}^*)$ in (12) yields:

$$\dot{e}_1 = \dot{\bar{u}}_{pv} - \left(\frac{\bar{i}_{pv}}{c_1} - \frac{i_{L1} + e_2}{c_1}\right)$$

which, together with (10), gives:

$$\dot{e}_1 = -k_1.e_1 + \frac{e_2}{c_1} \tag{16}$$

Step 2. Let us investigate the behavior of error variable e_2.

In view of (15) and (4), time-derivation of e_2 turns out to be:

$$\dot{e}_2 = \dot{i}_{L_1} - \dot{i}_{L_1}^* = \frac{\bar{u}_{pv}}{L_1} - \frac{\alpha_0.v_b}{L_1} - \dot{i}_{L_1}^* \tag{17}$$

From (10) one gets:

$$\dot{\beta}_1 = \dot{i}_{L_1}^* = -k_1.c_1.\dot{e}_1 + \dot{\bar{i}}_{pv} - c_1.\ddot{u}_{pv}^* \tag{18}$$

which together with (17) implies:

$$\dot{e}_2 = \frac{\bar{u}_{pv}}{L_1} - \frac{\alpha_0.v_b}{L_1} + k_1.c_1.\dot{e}_1 - \dot{\bar{i}}_{pv} + c_1.\ddot{u}_{pv}^* \tag{19}$$

In the new coordinates (e_1,e_2), the controlled system (3)-(4) is expressed by the couple of equations (16) and (19). We now need to select a Lyapunov function for such a system. As the objective is to drive its states (e_1,e_2) to zero, it is natural to choose the following function:

$$V_1 = \frac{1}{2}.e_1^2 + \frac{1}{2}.e_2^2 \tag{20}$$

The time-derivative of the latter, along the (e_1,e_2) trajectory, is:

$$\begin{aligned}\dot{V}_1 &= e_1.\dot{e}_1 + e_2.\dot{e}_2 \\ \dot{V}_1 &= -k_1.e_1^2 - k_2.e_2^2 + \\ & e_2.\left[\frac{\bar{u}_{pv}}{L_1} - \frac{\alpha_0.v_b}{L_1} + k_1.c_1.\dot{e}_1 - \dot{\bar{i}}_{pv} + c_1.\ddot{u}_{pv}^* + k_2.e_2\right]\end{aligned} \tag{21}$$

Where $k_2 > 0$ is a design parameter and $\dot{e}_2$ is to be replaced by the right side of (19). Equation (21) shows that the equilibrium $(e_1,e_2)=(0,0)$ is globally asymptotically stable if the term between brackets in (21) is set to zero. So doing, one gets the following control law:

$$\alpha_0 = \frac{L_1}{v_b}\left[\frac{\bar{u}_{pv}}{L_1} + k_1.c_1.\dot{e}_1 - \dot{\bar{i}}_{pv} + c_1.\ddot{u}_{pv}^* + k_2.e_2\right] \tag{22}$$

B. *Control of VCI inverter*

This controller consists of an inner current loop and an outer voltage loop. The inner current loop is responsible of producing the averaging value of switched control signal. The outer voltage loop assures a steady-state maximum input-output energy transfer ratio and regulate a desired steady-state output voltage that supply a resistive load [9].

Step 1. Let us introduce the input error:

$$e_3 = v_k - v_k^* \tag{23}$$

Where v_k^* is a reference signal of the output voltage.
Deriving e_3 with respect to time and accounting for (4) implies:

$$\dot{e}_3 = \dot{\bar{v}}_k - \dot{v}_k^* = \frac{\bar{i}_k - \bar{i}_{rk}}{c_2} - \dot{v}_k^* \tag{24}$$

In equation (24), $\bar{i}_k$ behaves as a virtual control input.
Such an equation shows that one gets $\dot{e}_3=-k_3.e_3$ ($k_3>0$ being a design parameter) provided that:

$$\bar{i}_k = -c_2.k_3.e_3 + c_2.\dot{v}_k^* + i_{rk} \tag{25}$$

As $\bar{i}_k$ is just a variable and not (an effective) control input, (25) cannot be enforced for all t≥0. Nevertheless, equation (25) shows that the desired value for the variable i_k is:

$$\bar{i}_k^* = -c_2.k_3.e_3 + c_2.\dot{v}_k^* + i_{rk} \tag{26}$$

Indeed, if the error:

$$e_4 = \bar{i}_k - i_k^* \tag{27}$$

Now, replacing (27) in (24) yields:

$$\dot{e}_3 = \frac{(e_4 + i_k^*) - \bar{i}_{rk}}{c_2} - \dot{v}_k^* \tag{28}$$

which, together with (26), gives:

$$\dot{e}_3 = -k_3.e_3 + \frac{e_4}{c_2} \tag{29}$$

Step 2. Let us investigate the behavior of error variable e_4.
In view of (6), time-derivation of e_2 turns out to be:

$$\dot{e}_4 = \dot{\bar{i}}_k - \dot{i}_k^* = \frac{\bar{v}_{sk} - \bar{v}_k - \bar{v}_{nm}}{L_2} - \dot{i}_k^* \tag{30}$$

From (7) one gets:

$$\dot{e}_4 = \frac{\alpha_k.\bar{v}_b - \bar{v}_k - \bar{v}_{nm}}{L_2} - \dot{i}_k^* \tag{31}$$

which together with (26) implies:

$$\dot{e}_4 = \frac{\alpha_k.\bar{v}_b - \bar{v}_k - \bar{v}_{nm}}{L_2} - \left[c_2.\dot{v}_k^* + \dot{i}_{rk} - c_2.k_3.\dot{e}_3\right] \tag{32}$$

In the new coordinates (e_3,e_4), the controlled system is expressed by the couple of equations (29) and (32). We now need to select a Lyapunov function for such a system. As the objective is to drive its states (e_3,e_4) to zero, it is natural to choose the following function:

$$V_2 = \frac{1}{2}.e_3^2 + \frac{1}{2}.e_4^2 \tag{33}$$

The time-derivative of the latter, along the (e_3,e_4) trajectory is:

$$\dot{V}_2 = e_3.\dot{e}_3 + e_4.\dot{e}_4$$

$$\dot{V}_2 = -k_3.e_3^2 - k_4.e_4^2$$

$$+e_4.\left[\frac{e_3}{c_2} + \frac{\alpha_k.\bar{v}_b - \bar{v}_k - \bar{v}_{nm}}{L_2} - c_2.\dot{v}_k^* - \dot{i}_{rk} + c_2k_3\dot{e}_3 + k_4e_4\right] \tag{34}$$

where $k_4>0$ is a design parameter. Equation (34) shows that the equilibrium (e_3,e_4)=(0,0) is globally asymptotically stable if the term between brackets in (34) is set to zero. So doing, one gets the following control law:

$$\alpha_k = \frac{L_2}{\bar{v}_b}\left[-\frac{e_3}{c_2} + \frac{\bar{v}_k + \bar{v}_{nm}}{L_2} + c_2.\dot{v}_k^* + \dot{i}_{rk} - c_2.k_3.\dot{e}_3 - k_4.e_4\right] \tag{35}$$

Where k =1, 2 or 3.

IV. Simulation result

The PV model, boost converter, buck inverter model, and non-linear controller are implemented in Matlab/Simulink. In the study, RSM-60 PV module has been selected as PV power source and the parameter of the components are chosen to deliver maximum 1.8kW of power generated by connecting 30 module of RSM-60 in parallel. The specification of the system and PV module are respectively summarized in following table.

TABLE I MAIN CHARACTERISTICS OF THE PV GENERATION SYSTEM

Parameters		Value
PV generator	P_{max}	60W
	u_{pv} à	16V
	P_{max}	21.5V
	V_{oc}	3.8A
	I_{cc}	
Boost converter	C_1	220µF
	L_1	0.004H
Inverter and load	v_b	450V
	L_2	0.001H
	c_2	10µF
	R	30Ω
Backstepping Controller	K_1	150
	k_2	10
	k_3	1000
	k_4	150000

Figure 5 shows the simulation results of the designed inverter when the solar radiation changes from 1000W/m^2 to 500W/m^2. Notice that according to figure 6 the maximum power point is reached after a smooth transient response according to radiation change. The output voltages of the inverter that supply the load are regulated to the reference (frequency=50Hz, Rms =220V) with low distortion. This distortion can be corrected by adjusting the parameters of controller.

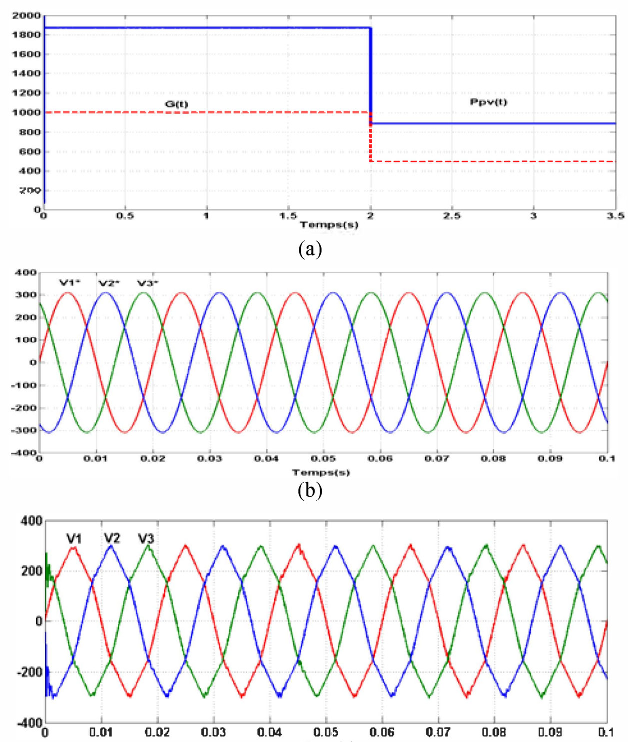

(c)

Figure. 5. (a) radiation and power, (b) reference of output voltage, (c) output voltage

V. Conclusions

A backstepping control strategy has been developed for a solar generating system to extract and inject the power extracted from a photovoltaic array and obtain regulated voltages that supply a resistive load in varying weather conditions. A desired array voltage is designed online using an MPPT searching algorithm to seek the unknown optimal array voltage. To track the designed trajectory, a tracking controller is developed to modulate the duty cycle of the boost converter and the inverter. The proposed controller is proven to yield global asymptotic stability with respect to the tracking errors via Lyapunov analysis. Simulation results are provided to verify the effectiveness of this approach.

References

[1] G. Ertasgin, D.M. Whaley, N. Ertugrul and W.L. Soong , A Current-Source Grid-Connected Converter Topology for Photovoltaic Systems, Australasian Universities Power Engineering Conference, 2006, Melbourne, Australia.

[2] N. Femia, G. Petrone, G. Spagnuolo, and M. Vitelli, “Optimization of Perturb and Observe maximum power point tracking method,” Power Electronics, IEEE Transactions , pp. 963–973, 2005.

[3] Jae Ho Lee; HyunSu Bae; Bo Hyung Cho; Sch. of Electr. Eng., Seoul Nat. Univ, ’’Advanced Incremental Conductance MPPT Algorithm with a Variable Step Size’’, Power Electronics and Motion Control Conference EPE-PEMC 12th International , 2006.

[4] Trishan Esram,, Patrick L. Chapman, Comparison of Photovoltaic Array Maximum Power Point Tracking Techniques , IEEE Transaction on Energie Conversion, VOL. 22, NO. 2, JUNE 2007, pp 439 – 449

[5] H. Abouobaida, M. Cherkaoui, M. Ouassaid, “Robust maximum power point tracking for photovoltaic cells: A backstepping mode control approach”, International Conference on Multimedia Computing and Systems (ICMCS), 2011 , pp. 1 – 4, 2011

[6] Marcelo Gradella Villalva, Jonas Rafael Gazoli, and Ernesto Ruppert Filho , Comprehensive Approach to Modeling and Simulation of Photovoltaic Arrays , IEEE Transaction On Power Electronics, vol. 24, NO. 5, May 2009, pp : 1198 – 1208

[7] Campbell, R.C. A Circuit-based Photovoltaic Array Model for Power System Studies , Power Symposium , NAPS '07. 39th North American, December 2007 , pp : 97 – 101

[8] Hong Wang; Donglai Zhang; The Stand-alone PV Generation System with Parallel Battery Charger, International Conference On Electrical and Control Engineering (ICECE), 2010, pp: 4450 - 4453

[9] Hong Wang; Bing Li; The cooperated MPPT control of stand-alone PV Power generation system, World Congress on Intelligent Control and Automation (WCICA), 2010, pp: 2228 - 2231